

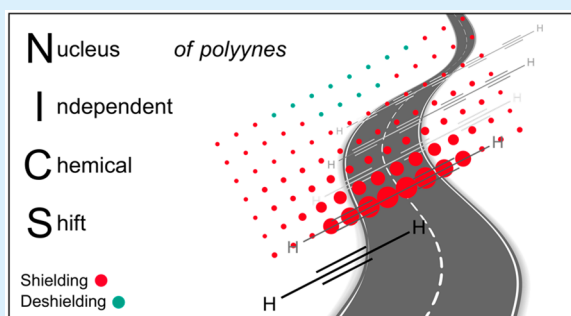
Origin of Shielding and Deshielding Effects in NMR Spectra of Organic Conjugated Polyynes

Andreas Ehnbom,^{ID} Michael B. Hall,^{*,ID} and John A. Gladysz^{*,ID}

Department of Chemistry, Texas A&M University, P.O. Box 30012, College Station, Texas 77843-3012, United States

 Supporting Information

ABSTRACT: Nucleus independent chemical shifts (NICS) for conjugated polyynes $H(C\equiv C)_nH$ are reported ($n = 2-10$). There is marked shielding within the carbon chain, gradually decreasing with radial distance and transitioning to a weakly deshielding region at $2.5-3.0 \text{ \AA}$, as well as other trends. Interestingly, the magnitude of the shielding is only very weakly dependent upon the chain length or distance from the termini. ^1H and ^{13}C NMR chemical shifts are also computed and the trends analyzed.



In previous generations, chemists were taught that “ring currents” were largely responsible for NMR shielding and deshielding phenomena associated with benzene, ethyne (acetylene), and derivatives thereof.^{1,2} The models traditionally employed are depicted in Figure 1. They offered intuitively plausible rationales for the deshielding of benzene protons (I) and the shielding of ethyne protons (II), as well as effects in certain types of derivatives. For example, two of the sp^3 protons of [7]paracyclophane (**1**), in which the methylene chain must closely hug the π face of the *p*-phenylene moiety, exhibit markedly upfield ^1H NMR signals at -0.3 to -0.9 ppm (δ , CCl_4).³ These models also gained currency in their apparent applicability to nonbenzenoid aromatic systems, such as 9,10-dihydropyrenes.⁴ They also begged the question as to possible cumulative effects in one-dimensional arrays, such as $[n,n]$ -paracyclophanes and conjugated polyynes.

However, subsequent computational studies have shown models I and II to be erroneous.⁵ These feature calculations and

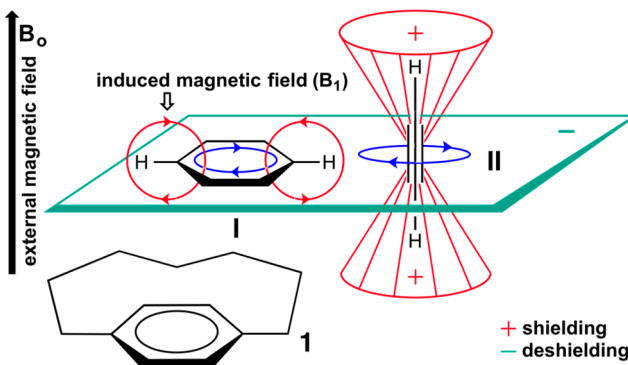


Figure 1. Classical ring-current-based shielding/deshielding models for benzene (I) and ethyne (II).^{1,2}

analyses of “nucleus independent chemical shifts” or “NICS” associated with the three-dimensional space surrounding benzene and ethyne. The resulting chemical shift “maps” or grid plots, depicted in Figure 2, show pronounced shielding regions (red spheres) (1) within and above the benzene ring and (2) within the $\text{HC}\equiv\text{CH}$ linkage or along immediately adjacent vectors.

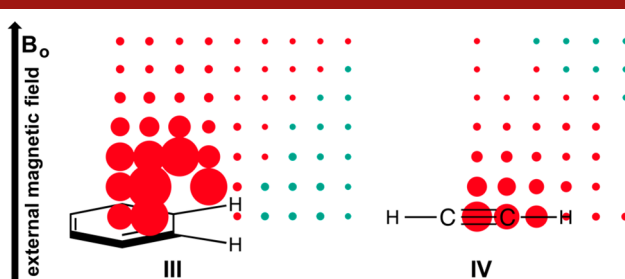


Figure 2. Computed NICS about benzene (III) and ethyne (IV), with red and green spheres indicating shielding and deshielding, respectively. The data are from ref 5, which can be consulted for the scales represented by the spheres.

The deshielding regions (green spheres) are comparatively modest, occurring at significant radial extensions from the benzene ring and $\text{HC}\equiv\text{CH}$ axis. The patterns are clearly inconsistent with ring current models.⁶

We have had a long-standing interest in the physical and chemical properties of extended polyynes that are capped on one or both termini by transition metal fragments.^{7–9} These have the general formula $L_yM(C\equiv C)_nZ$ ($Z = \text{SiR}_3, \text{H}$) and $L_yM(C\equiv C)_nML_y$. A typical example of the latter is given in Figure 3 (2).^{8b}

Received: December 13, 2018

Published: January 18, 2019

These have more recently been expanded to include rotaxanes such as 3.⁹

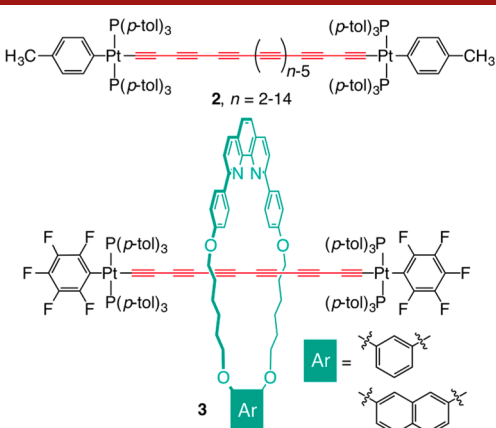


Figure 3. Representative diplatinum polyynediyl complexes.

The interpretation of the NMR properties of such assemblies—which also have been of interest in several other research groups^{10–13}—requires that the shielding and deshielding regions, and their attendant magnitudes, of organic polyynes be precisely defined. Surprisingly, to our knowledge, there have been no NICS studies of simple acyclic 1,3-diyne, 1,3,5-triyne, or any higher homologues.¹⁴ In this letter, this conspicuous gap is addressed for the doubly terminal organic polyynes $\text{H}(\text{C}\equiv\text{C})_n\text{H}$ ($n = 2–10$).

The NICS values for the polyynes $\text{H}(\text{C}\equiv\text{C})_n\text{H}$ were computed using standard protocols.¹⁵ The full results are presented in the Supporting Information (SI), and data for three representative substrates are depicted in Figure 4. As is easily seen, there is marked shielding (1) within and (2) proximal to the sp carbon chain or $(\text{C}\equiv\text{C})_n$ segment. This tails off with the

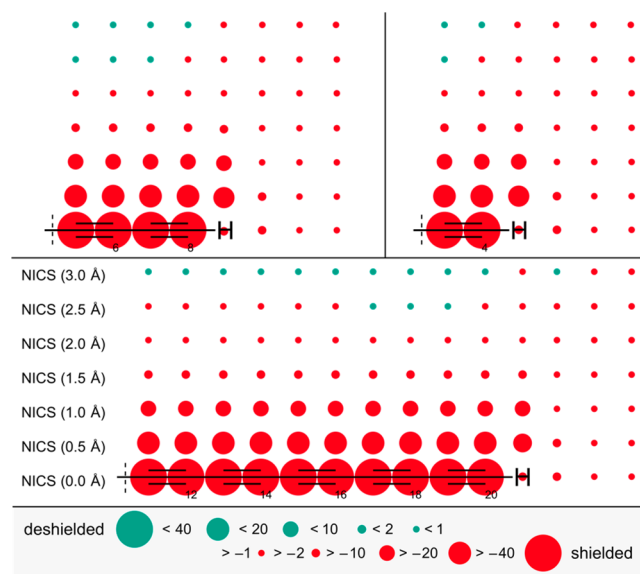


Figure 4. Representative NICS grid plots for ethyne and the diterminal polyynes $\text{H}(\text{C}\equiv\text{C})_n\text{H}$ ($n = 2–10$). The distances are not to scale. The grid points on the y axis represent increments of 0.50 \AA , and those on the x axis represent increments of $1.19–1.21$ or $1.35–1.37 \text{ \AA}$ (for $\text{C}\equiv\text{C}$ and $\equiv\text{C}-\text{C}\equiv$ linkages, respectively) or $1.06–1.11 \text{ \AA}$ (for $\text{C}-\text{H}$ linkages and points extending further out from the carbon chain).

radial distance, and eventually a very slightly deshielded region is reached ($2.5–3.0 \text{ \AA}$).

The most important conclusion is that the magnitude of the shielding at any distance is essentially *independent of the sp carbon chain length and the position along the chain*. In other words, one encounters nearly the same NICS value regardless of the number of triple bonds or exact location along the $(\text{C}\equiv\text{C})_n$ segment. There are no additive or multiplicative effects.

The same holds as the one-dimensional vectors defined by or parallel to the sp carbon chains are extended. As shown in Figure 4, the shielding found at the hydrogen atoms is markedly attenuated. However, at radial extensions of $0.5–2.0 \text{ \AA}$, the diminution is not as pronounced. When grid points further out on the $\text{H}(\text{C}\equiv\text{C})_n\text{H}$ axes are sampled, the degree of shielding gradually decreases. This same trend is found when the grid is radially extended.

These results indicate that, in rotaxanes derived from organic polyynes, the ^1H and ^{13}C NMR chemical shifts of the mechanically linked macrocycles are not *directly* affected by the sp carbon chain lengths. However, these chemical shifts will be influenced by the distances of the macrocycle nuclei from the end groups, which will, in turn, be affected by the sp carbon chain length. This will be the principal origin of any chemical shift trends as the sp carbon chain lengths are varied.

In the course of calculating the NICS grids for the diterminal polyynes $\text{H}(\text{C}\equiv\text{C})_n\text{H}$, chemical shifts for the hydrogen and carbon atoms were also obtained. Although such compounds become unstable at moderate chain lengths, some experimental data are available^{16–19} and are presented in Figures 5 and 6. For

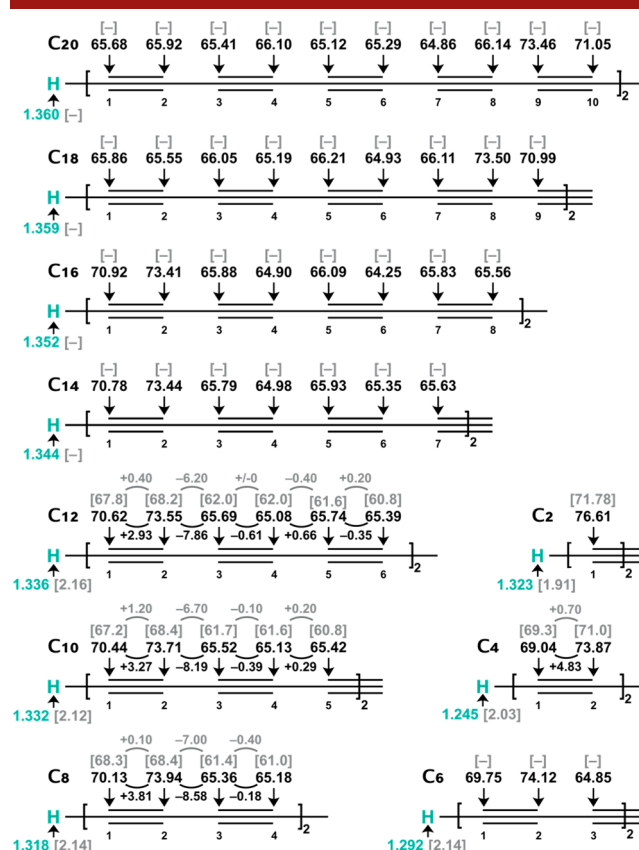


Figure 5. Computed ^1H and ^{13}C NMR chemical shifts of ethyne and the diterminal polyynes $\text{H}(\text{C}\equiv\text{C})_n\text{H}$ vs TMS and (when available) experimental values [in brackets].

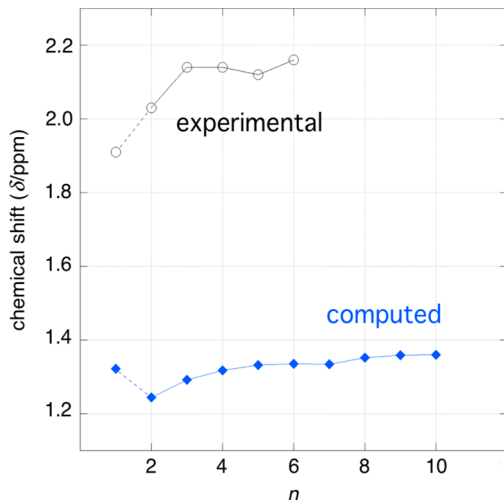


Figure 6. Computed ^1H NMR chemical shifts for ethyne and the diterminal polyynes $\text{H}(\text{C}\equiv\text{C})_n\text{H}$ vs TMS (blue rhomb) and experimental values (open circle).

the calculated values, there is a monotonic downfield shift from δ 1.245 to 1.360 as n is extended from 2 (1,3-butadiyne) to 10 (1,3,5,7,9,11,13,15,17,19-eicosadecayne). From the slope in Figure 6, the value for eicosadecayne (δ 1.360) appears to be close to an asymptotic limit, such that there would be little change in still longer polyynes. For the experimental values ($n = 2\text{--}6$), there is a general downfield trend, but—perhaps due to the different solvents employed^{16–19} and experimental error—the shifts are very close for $n = 3\text{--}6$ (δ 2.12 to 2.16).

As can readily be seen in Figure 6, the ^1H chemical shift computed for ethyne is downfield from that of 1,3-butadiyne, as opposed to the upfield value that would have been extrapolated from the other data points. This discontinuity is not necessarily surprising as ethyne (with $n = 1$) is not a polyyne. There is a hydrogen atom on the opposite end of the triple bond from the $\text{HC}\equiv$ group, as opposed to an sp carbon atom in the higher homologues. However, the experimental ^1H NMR chemical shift of ethyne (δ 1.91 ppm in CDCl_3 in two studies)¹⁶ is upfield of those of 1,3-butadiyne and 1,3,5-hexatriyne. In the absence of any experimental artifact, it must be concluded that the computations fail to model this one datum.²⁰ Nonetheless, a variety of benchmarking computations are provided in the SI that validate the methodology.

We were curious as to whether the preceding ^1H NMR chemical shift trends might be manifested in monoterinal conjugated polyynes $\text{R}(\text{C}\equiv\text{C})_n\text{H}$, which also become less stable at higher chain lengths.²¹ The most extensive series of data we could locate was for the series $\text{Tr}^*(\text{C}\equiv\text{C})_n\text{H}$ (4), where Tr^* denotes a hexakis(*t*-butyl)-substituted trityl group, as shown in Figure 7.^{11b} Tykwiński could obtain ^1H NMR spectra for $n = 1\text{--}7$. However, more than one solvent was employed, complicating comparisons (n , δ (ppm)/solvent: 1, 2.59/ CDCl_3 ; 2, 2.10/ CDCl_3 ; 3, 2.07/ CDCl_3 ; 4, 2.07/ CDCl_3 ; 5, 2.26/ CD_2Cl_2 ; 6, 2.11/ CDCl_3 ; 7, 2.23/ CD_2Cl_2).^{11b} A less extensive series of aryl substituted terminal polyynes (5, Figure 7) exhibited a nicely monotonic upfield trend as n increased from 1 to 4 (δ (ppm)/ CDCl_3 3.20, 2.54, 2.31, 2.23).²¹

The ^{13}C NMR chemical shifts computed for $\text{H}(\text{C}\equiv\text{C})_n\text{H}$ are plotted in Figure 8. As n is extended from 2 to 10, the chemical shifts of the terminal carbon atoms (C1) shift monotonically to lower fields.

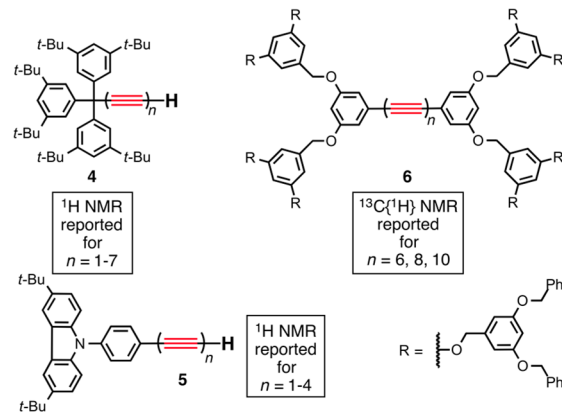


Figure 7. Organic conjugated polyynes used for chemical shift comparisons.^{11a,b,21}

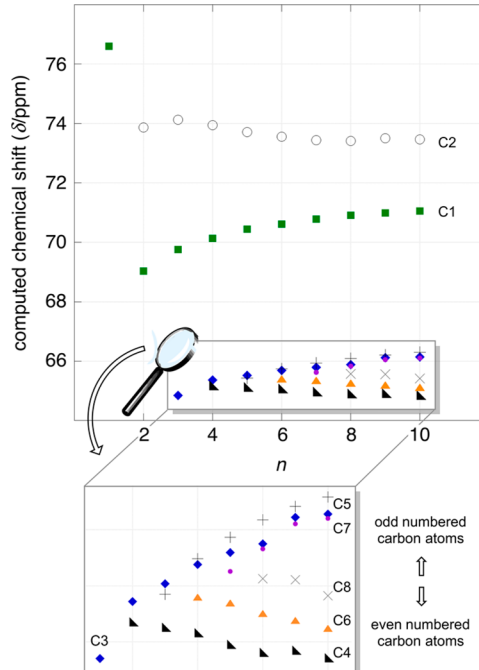


Figure 8. Computed ^{13}C NMR chemical shifts for ethyne and the diterminal polyynes $\text{H}(\text{C}\equiv\text{C})_n\text{H}$ ($\text{HC}_1\equiv\text{C}_2\text{--}\text{C}_3\equiv\text{C}_4\cdots$) vs TMS as a function of n (green square = C1; open circle = C2; blue rhomb = C3; black triangle = C4; black plus sign = C5; orange triangle = C6; purple filled circle = C7; black cross = C8).

As was seen with the computed ^1H NMR chemical shifts, ethyne ($n = 1$) presents an exception to the monotonic trend exhibited by the higher homologues. The shift computed for C2 of 1,3-butadiyne also slightly deviates from an analogous monotonic trend. Interestingly, the chemical shifts of the “odd numbered carbon atoms” (C1, C3, C5, etc.) move downfield with increasing chain length, but those of the “even numbered carbon atoms” (C2, C4, etc.) move upfield. Overall, the chemical shift trends are in general but not perfect agreement with those found experimentally for 1,3-butadiyne, 1,3,5,7-octatetrayne, 1,3,5,7,9-decapentayne, and 1,3,5,7,9,11-dodecahexayne ($n = 2, 4, 5, 6$; Figure 5).

We were also curious as to whether the preceding ^{13}C NMR chemical shift trends might be manifested in nonterminal organic conjugated polyynes. Hirsch has characterized a series of polyynes $\text{Ar}^*(\text{C}\equiv\text{C})_n\text{Ar}^*$ (6; $n = 6, 8, 10$) in which Ar^* denotes

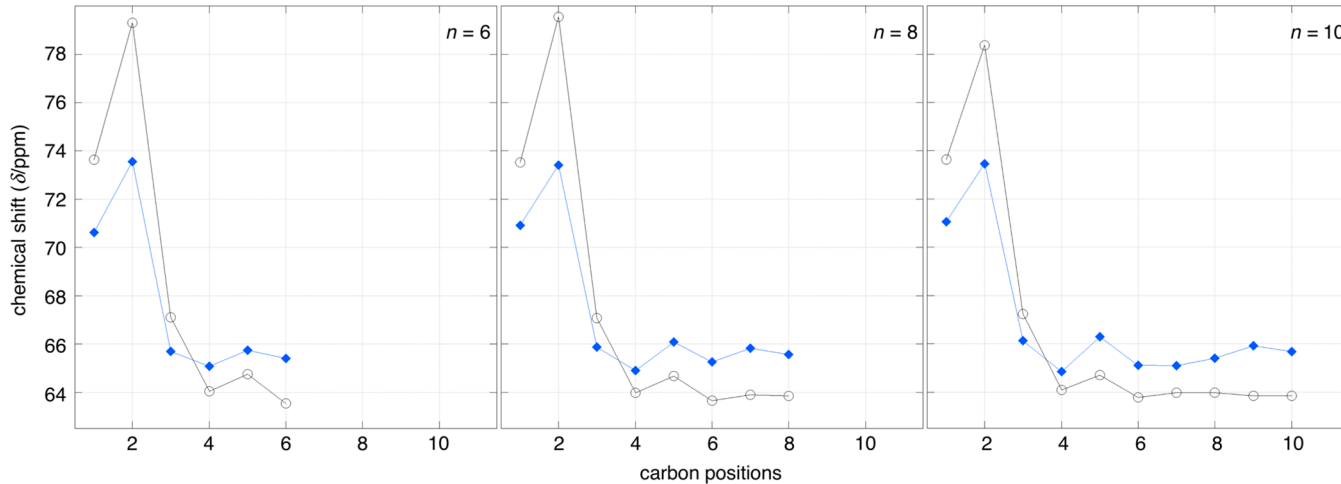


Figure 9. Correlation of ^{13}C NMR chemical shifts trends computed for $\text{H}(\text{C}\equiv\text{C})_n\text{H}$ (blue diamond) vs those observed experimentally for $\text{Ar}^*(\text{C}\equiv\text{C})_n\text{Ar}^*$ (6; open circle; acetone- d_6). The C7/C8 and C9/C10 signals of $\text{Ar}^*(\text{C}\equiv\text{C})_{10}\text{Ar}^*$ were reported as overlapping singlets at δ 63.97 and 63.84 ppm, respectively.

a dendrimer like aryl end group (Figure 7).^{11a} As summarized in Figure 9, his experimental data (recorded in acetone- d_6) strikingly mirror the computed trends, providing further validation of the methodology. Tykwinski also studied an extensive series of polyynes $\text{Tr}^*(\text{C}\equiv\text{C})_n\text{Tr}^*$ derived from the oxidative coupling of 4^{11b} and conducted ^{13}C labeling studies with other substrates to secure NMR assignments.²² However, the correlations with his ^{13}C NMR spectra ($n = 4, 6, 8, 10$; recorded in CDCl_3) were weaker. In this context, it should be noted that the ^{13}C NMR signals of long polyynes can be challenging to observe for a number of well-understood reasons, including decreased solubility with chain length, rendering the chemical shifts subject to greater experimental error. Also, as noted by a reviewer, the non-hydrogen end groups introduce electronic interactions with the sp carbon chain that are not represented in our calculations.

In conclusion, the NICS grids associated with the doubly terminal conjugated polyynes $\text{H}(\text{C}\equiv\text{C})_n\text{H}$ do not exhibit any special additive or multiplicative effects or vestiges of the old ring current model (Figure 1). In other words, the degrees of shielding or deshielding encountered in a radial direction perpendicular to the $(\text{C}\equiv\text{C})_n$ linkages are essentially identical, irrespective of the number of the triple bonds and the position or location along the $(\text{C}\equiv\text{C})_n$ linkages. This has significant implications for interpreting the NMR data of conjugated polyynes that engage in mechanical bonding, such as rotaxanes. Finally, the data from these calculations can also be useful in assigning the ^{13}C NMR signals of conjugated polyynes.

■ ASSOCIATED CONTENT

§ Supporting Information

The Supporting Information is available free of charge on the ACS Publications website at DOI: [10.1021/acs.orglett.8b03990](https://doi.org/10.1021/acs.orglett.8b03990).

Additional computational data (exact NICS values, array of all NICS grid plots, methodological details, and validation experiments) (PDF)

Optimized structures (XYZ)

NICS input structures (XYZ)

■ AUTHOR INFORMATION

Corresponding Authors

*E-mail: hall@chem.tamu.edu.

*E-mail: gladysz@chem.tamu.edu.

ORCID ®

Andreas Ehnbohm: [0000-0002-7044-1712](https://orcid.org/0000-0002-7044-1712)

Michael B. Hall: [0000-0003-3263-3219](https://orcid.org/0000-0003-3263-3219)

John A. Gladysz: [0000-0002-7012-4872](https://orcid.org/0000-0002-7012-4872)

Notes

The authors declare no competing financial interest.

■ ACKNOWLEDGMENTS

We thank the U.S. National Science Foundation (CHE-1566601 and CHE-1664866) for financial support, the Laboratory for Molecular Simulation and Texas A&M High Performance Research Computing Facility for computational resources, and Dr. Lisa M. Pérez (Texas A&M University) for helpful discussions.

■ REFERENCES

- (1) Johnson, C. E., Jr.; Bovey, F. A. Calculation of Nuclear Magnetic Resonance Spectra of Aromatic Hydrocarbons. *J. Chem. Phys.* **1958**, *29*, 1012–1014.
- (2) Du Vernet, R.; Boekelheide, V. Nuclear Magnetic Resonance Spectroscopy. Ring-Current Effects on Carbon-13 Chemical Shifts. *Proc. Natl. Acad. Sci. U. S. A.* **1974**, *71*, 2961–2964.
- (3) Wolf, A. D.; Kane, V. V.; Levin, R. H.; Jones, M., Jr. [7]Paracyclophane. *J. Am. Chem. Soc.* **1973**, *95*, 1680–1680.
- (4) Mitchell, R. H.; Chen, Y.; Khalifa, N.; Zhou, P. The Synthesis, Aromaticity, and NMR Properties of [14]Annulene Fused Organometallics. Determination of the Effective Bond Localizing Ability (“Relative Aromaticity”) and Diamagnetic Anisotropy of Several Organometallic Moieties. *J. Am. Chem. Soc.* **1998**, *120*, 1785–1794 and earlier work cited therein.
- (5) Wannere, C. S.; Schleyer, P. v. R. How Do Ring Currents Affect ^1H NMR Chemical Shifts? *Org. Lett.* **2003**, *5*, 605–608 and earlier work by others cited therein.
- (6) Nonetheless, contributions from classical ring currents continue to be considered in various contexts: Pelloni, S.; Lazzaretti, P. Ring current models for acetylene and ethylene molecules. *Chem. Phys.* **2009**, *356*, 153–163.

(7) Dembinski, R.; Bartik, T.; Bartik, B.; Jaeger, M.; Gladysz, J. A. Toward Metal-Capped One-Dimensional Carbon Allotropes: Wirelike C_6 – C_{20} Polyy nediy Chains that Span Two Redox-Active (η^5 - C_5Me_5) $Re(NO)(PPh_3)$ Endgroups. *J. Am. Chem. Soc.* **2000**, *122*, 810–822 and earlier work cited therein.

(8) (a) Mohr, W.; Stahl, J.; Hampel, F.; Gladysz, J. A. Synthesis, Structure, and Reactivity of sp Carbon Chains with Bis(phosphine) Pentafluorophenylplatinum Endgroups: Butadiynediyl (C_4) through Hexadeca octaynediy (C_{16}) Bridges, and Beyond. *Chem. - Eur. J.* **2003**, *9*, 3324–3340. (b) Zheng, Q.; Bohling, J. C.; Peters, T. B.; Frisch, A. C.; Hampel, F.; Gladysz, J. A. A Synthetic Breakthrough into an Unanticipated Stability Regime: A Series of Isolable Complexes in which C_6 , C_8 , C_{10} , C_{12} , C_{16} , C_{20} , C_{24} , and C_{28} Polyy nediy Chains Span Two Platinum Atoms. *Chem. - Eur. J.* **2006**, *12*, 6486–6505.

(9) (a) Weisbach, N.; Baranová, Z.; Gauthier, S.; Reibenspies, J. H.; Gladysz, J. A. A new type of insulated molecular wire: a rotaxane derived from a metal-capped conjugated tetrayne. *Chem. Commun.* **2012**, *48*, 7562–7564. (b) Baranová, Z.; Amini, H.; Bhuvanesh, N.; Gladysz, J. A. Rotaxanes Derived from Dimetallic Polyy nediy Complexes: Extended Axles and Expanded Macrocycles. *Organometallics* **2014**, *33*, 6746–6749.

(10) See also: Bruce, M. I.; Zaitseva, N. N.; Nicholson, B. K.; Skelton, B. W.; White, A. H. Syntheses and molecular structures of some compounds containing many-atom chains end-capped by tricobalt carbonyl clusters. *J. Organomet. Chem.* **2008**, *693*, 2887.

(11) Contemporary research groups active with organic conjugated polyynes: (a) Gibtner, T.; Hampel, F.; Gisselbrecht, J.-P.; Hirsch, A. End-Cap Stabilized Oligoynes: Model Compounds for the Linear sp Carbon Allotrope Carbyne. *Chem. - Eur. J.* **2002**, *8*, 408–432 and earlier work cited therein. (b) Chalifoux, W. A.; Tykwiński, R. R. Synthesis of polyynes to model the sp-carbon allotrope carbyne. *Nat. Chem.* **2010**, *2*, 967–971 and earlier work cited therein. (c) Kohn, D. R.; Gawel, P.; Xiong, Y.; Christensen, K. E.; Anderson, H. L. Synthesis of Polyynes Using Dicobalt Masking Groups. *J. Org. Chem.* **2018**, *83*, 2077–2086.

(12) Other studies of rotaxanes based upon conjugated polyynes: (a) Saito, S.; Takahashi, E.; Nakazono, K. Synthesis of [2]Rotaxanes by the Catalytic Reactions of a Macroyclic Copper Complex. *Org. Lett.* **2006**, *8*, 5133–5136. (b) Movsisyan, L. D.; Franz, M.; Hampel, F.; Thompson, A. L.; Tykwiński, R. R.; Anderson, H. L. Polyyne Rotaxanes: Stabilization by Encapsulation. *J. Am. Chem. Soc.* **2016**, *138*, 1366–1376 and earlier work cited therein.

(13) Catenanes that contain conjugated polyynes: (a) Dietrich-Buchecker, C. O.; Khemiss, A.; Sauvage, J.-P. High-yield Synthesis of Multiring Copper(I) Catenates by Acetylenic Oxidative Coupling. *J. Chem. Soc., Chem. Commun.* **1986**, 1376–1378. (b) Dietrich-Buchecker, C. O.; Hemmert, C.; Khémis, A.-K.; Sauvage, J.-P. Synthesis of Dicopper [3]-Catenates and [3]-Catenands by Acetylenic Oxidative Coupling. Preparation and Study of Corresponding Homodimetallic [3]-Catenates (Ag^+ , Zn^{2+} , Co^{2+} , and Ni^{2+}). *J. Am. Chem. Soc.* **1990**, *112*, 8002–8008. (c) Hamilton, D. G.; Sanders, J. K. M.; Davies, J. E.; Clegg, W.; Teat, S. Neutral [2]catenanes from oxidative coupling of π -stacked components. *Chem. Commun.* **1997**, 897–898. (d) Hamilton, D. G.; Feeder, N.; Prodi, L.; Teat, S. J.; Clegg, W.; Sanders, J. K. M. Tandem Hetero-Catenation: Templating and Self-Assembly in the Mutual Closure of Two Different Interlocking Rings. *J. Am. Chem. Soc.* **1998**, *120*, 1096–1097. (e) Hamilton, D. G.; Prodi, L.; Feeder, N.; Sanders, J. K. M. Synthesis of macrocycles and an unusually asymmetric [2]catenane via templated acetylenic couplings. *J. Chem. Soc., Perkin Trans. 1* **1999**, *1*, 1057–1065. (f) Duda, S.; Godt, A. The Effect of Ring Size on Catenane Synthesis. *Eur. J. Org. Chem.* **2003**, *2003*, 3412–3420. (g) Gunter, M. J.; Farquhar, S. M. Neutral π -associated porphyrin [2]catenanes. *Org. Biomol. Chem.* **2003**, *1*, 3450–3457. (h) Miljanić, O. Š.; Dichtel, W. R.; Mortezaei, S.; Stoddart, J. F. Cyclobis(paraquat-p-phenylene)-Based [2]Catenanes Prepared by Kinetically Controlled Reactions Involving Alkynes. *Org. Lett.* **2006**, *8*, 4835–4838. (i) Miljanić, O. Š.; Dichtel, W. R.; Khan, S. I.; Mortezaei, S.; Heath, J. R.; Stoddart, J. F. Structural and Co-conformational Effects of Alkyne-Derived Subunits in Charged Donor-Acceptor [2]-Catenanes. *J. Am. Chem. Soc.* **2007**, *129*, 8236–8246. (j) Sato, Y.; Yamasaki, R.; Saito, S. Synthesis of [2]Catenanes by Oxidative Intramolecular Diyne Coupling Mediated by Macroyclic Copper(I) Complexes. *Angew. Chem., Int. Ed.* **2009**, *48*, 504–507. (k) Sato, Y.; Yamasaki, R.; Saito, S. Synthesis of [2]Catenanes by Oxidative Intramolecular Diyne Coupling Mediated by Macroyclic Copper(I) Complexes. *Angew. Chem.* **2009**, *121*, 512–515.

(14) However, the NICS associated with a currently unknown class of molecules, fully conjugated cyclic polyynes of the formulae C_6 , C_{10} , C_{14} , C_{18} , C_{22} , C_{26} , and C_{30} ($-(C\equiv C)_n-$), have been reported: Remya, K.; Suresh, C. H. Carbon rings: a DFT study on geometry, aromaticity, intermolecular carbon–carbon interactions and stability. *RSC Adv.* **2016**, *6*, 44261–44271.

(15) See the *Supporting Information* for all the computational details including validations of the methodology employed.

(16) 1H and ^{13}C NMR spectra of $HC\equiv CH$ (in $CDCl_3$): (a) Zuschneid, T.; Fischer, H.; Handel, T.; Albert, K.; Häfleger, G. Z. Experimental Gas Phase 1H NMR Spectra and Basis Set Dependence of *ab initio* GIAO MO Calculations of 1H and ^{13}C NMR Absolute Shieldings and Chemical Shifts of Small Hydrocarbons. *Z. Naturforsch., B: J. Chem. Sci.* **2004**, *59b*, 1153–1176 (see Table 2). (b) Abraham, R. J.; Reid, M. Proton chemical shifts in NMR. Part 16. Proton chemical shifts in acetylenes and the anisotropic and steric effects of the acetylene group. *J. Chem. Soc., Perkin Trans. 2* **2001**, *2*, 1195–1204.

(17) 1H NMR spectra of $H(C\equiv C)_nH$ ($n = 2, 3$; in $CDCl_3$): Kloster-Jensen, E. Preparation of Pure Triacetylene, Tetraacetylene, and Pentaacetylene and Investigation of Their Electronic Spectra. *Angew. Chem., Int. Engl.* **1972**, *11*, 438–439. Kloster-Jensen, E. Reindarstellung und Elektronenspektrum des Triacetylen, Tetraacetylen und Pentaacetylen. *Angew. Chem.* **1972**, *84*, 483–485.

(18) 1H and ^{13}C NMR spectra of $H(C\equiv C)_nH$ ($n = 4, 5, 6$; in $C_2D_2Cl_4$): Wakabayashi, T.; Tabata, H.; Doi, T.; Nagayama, H.; Okuda, K.; Umeda, R.; Hisaki, I.; Sonoda, M.; Tobe, Y.; Minematsu, T.; Hashimoto, K.; Hayashi, S. Resonance Raman spectra of polyyne molecules $C_{10}H_2$ and $C_{12}H_2$ in solution. *Chem. Phys. Lett.* **2007**, *433*, 296–300.

(19) ^{13}C NMR spectrum of $H(C\equiv C)_2H$: Kurosu, H.; Webb, G. A.; Ando, I. *Ab initio* ^{13}C Nuclear Shielding Calculations for Some Hydrocarbons using the GIAO Procedure. *Magn. Reson. Chem.* **1992**, *30*, 1122–1124.

(20) The use of implicit solvent models often give little improvement. However, explicit solvent models may potentially be more helpful, and promising new computational methodologies are becoming available. See for example: Stoychev, G. L.; Auer, A. A.; Neese, F. J. Efficient and Accurate Prediction of Nuclear Magnetic Resonance Shielding Tensors with Double-Hybrid Density Functional Theory. *J. Chem. Theory Comput.* **2018**, *14*, 4756–4771.

(21) Wang, C.; Batsanov, A. S.; West, K.; Bryce, M. R. Synthesis and Crystal Structures of Isolable Terminal Aryl Hexatriyne and Octatetrayne Derivatives: $Ar-(C\equiv C)_nH$ ($n = 3, 4$). *Org. Lett.* **2008**, *10*, 3069–3072.

(22) Tykwiński, R. R.; Luu, T. Synthesis and ^{13}C NMR Spectroscopy of ^{13}C -Labeled α,ω -Diphenylpolyynes. *Synthesis* **2012**, *44*, 1915–1922. Subtle “oscillations” in chemical shift trends noted by these authors are also manifested in our computational data.